WILEY

Application of parelectric spectroscopy to detect skin cancer—A pilot study

Frederike S. Arnold-Brüning[1] | Tobias Blaschke[2] | Klaus Kramer[2] | Jürgen Lademann[1] | Gisela Thiede[1] | Joachim W. Fluhr[1] | Alexa Patzelt[1] | Martina C. Meinke[1] 🆔

[1]Department of Dermatology, Venerology and Allergology, Center of Experimental and Applied Cutaneous Physiology, Charité—Universitätsmedizin Berlin, Corporate Member of Freie Universität Berlin, Humboldt-Universität zu Berlin and Berlin Institute of Health, Berlin, Germany

[2]Parelectrics, Berlin, Germany

Correspondence
Martina C. Meinke, Center of Experimental and Applied Cutaneous Physiology, Department of Dermatology, Venereology and Allergology, Charité—Universitätsmedizin Berlin, Berlin 10117, Germany.
Email: martina.meinke@charite.de

Abstract

Background: The early detection of skin cancer is still challenging and calls for objective, fast diagnostic, and ideally non-invasive methods in order to leave the potentially malignant tumor cells unaltered. In this paper, the parelectric spectroscopy was applied to evaluate the potential of a non-invasive detection of basal cell carcinoma (BCC) and malignant melanoma.

Materials and Methods: A prototype of parelectric spectroscopy was used to investigate non-invasively dipole density and mobility of suspicious skin lesions. The differences in investigated tissue were analyzed compared to pathohistological findings in a clinical study on 51 patients with suspected BCC and malignant melanoma.

Results: The non-invasive parelectric spectroscopy could differentiate between normal skin, BCC, and melanoma but failed to distinguish between different types of skin cancer. The data were normalized to unsuspected nearby skin because the different skin locations influence dipole density and mobility.

Conclusion: The results of the pilot study indicate that the parelectric spectroscopy might be an additional, useful non-invasive diagnostic procedure to distinguish between normal skin and skin cancer.

KEYWORDS
basal cell carcinoma, dipole density, dipole mobility, malignant melanoma

1 | INTRODUCTION

Skin cancer incidence is still increasing in Germany. Its early detection is very important to lower the risk of metastases and also to minimize scars and to improve the esthetic surgical outcome. The standard diagnostic procedure for suspicious individual lesions for non-melanoma skin cancer is a skin biopsy with a subsequent histopathologically analysis prior to any surgical intervention.[1-3] After tumor excision, the tumor margins are assessed and surgically corrected, if necessary. The histological results of hospitalized patients undergoing excision are available overnight. They are not dismissed before these results are known and the lesion completely removed. If the excision is performed in an outpatient facility, the lesion is closed after surgery entailing the risk of an additional surgery if the tumor margin is not free of tumor cells.

A device, which would be able to distinguish between normal tissue and tumorous tissue, could help to reduce the amount of false-positive cases and to minimize surgical intervention. In previous

[Correction added on 23 November 2020, after the first online publication: Projekt Deal funding statement has been added.]

studies, this could be shown using optical coherence tomography (OCT) or confocal laser scanning microscopy (RCM), when dermatoscopic findings were inconclusive.[4,5] Nevertheless, a method not being dependent on the experience of the investigator would be favorable. Spectroscopic methods such as Raman, multimodal imaging, and fluorescence methods were tested to distinguish between normal skin and skin cancer.[6-9] So far, these techniques have not been commercially available for clinical assessment of the skin. In the present study, parelectric spectroscopy as a new technique was investigated in a pilot study on 51 patients with 59 lesions suspicious for non-melanoma (45 lesions) and melanoma (14 lesions) skin cancer. So far, the parelectric spectroscopy has been used for structure and dynamical analysis of drug-carrier systems.[10-13]

The principle of this method is based on the high number of electric dipoles exist due to water or components of cell membranes in human tissue. The hypothesis is that the dipoles differ between the tissue types or for the same type between normal and malignant tissue. This difference is expected in density and mobility of the dipoles which can be measured by parelectric spectroscopy.

First measurements were performed on larynx tumor after excision.[14,15] These promising results led to the hypothesis that normal skin and skin cancer should be distinguishable, too. In the present pilot study, 51 patients with suspected BCC and melanoma were included and measured. The measurements were performed prior to surgery. The spectroscopic results were correlated with the histological findings.

2 | MATERIALS AND METHODS

2.1 | Subjects

The study was performed from April 2012 to August 2013 in accordance with the ethical guidelines of the Declaration of Helsinki. The study was approved by the ethics committee of Berlin (DIMDI No.:00018467, Eudamed No.: CIV-11-10-002625). All volunteers have given their informed written consent.

Only subjects over the age of 18 with suspicious skin lesions, that could be either a basal cell carcinoma or a malignant melanoma, were included into the study. All patients were scheduled for a surgical intervention (either biopsy or complete excision). The histopathology served as a reference. The lesions had to be accessible with the measurement probe. Exclusion criteria were other skin diseases in the same/nearby localization, pregnancy, and breastfeeding.

In total, 51 patients were subjected to 59 and 14 healthy volunteers to 24 measurements. Details are shown in Table 1.

2.2 | Parelectric spectroscopy

The parelectric spectroscopy investigates the response of dipoles to an applied external electric field dependent on the frequency. A short introduction to the theory will be given here, a more detailed description can be found, for example, in.[14]

Briefly, phospholipids are the main components of cell membranes of skin cells. The headgroups of these lipids constitute electrical dipoles which respond to an applied external electric ac-field. The device ParaScan I determines the complex permittivity depending on the frequency of this ac-field. The real part of represents the dispersion $\varepsilon'(f)$ and the imaginary part the absorption $\varepsilon''(f)$. Both quantities can be described by Debye' relations,[16]

$$\varepsilon'(f) = e_\infty + \frac{\Delta\varepsilon}{1 + \left(\frac{f}{f_0}\right)^2},$$

$$\varepsilon''(f) = \frac{\sigma}{2\pi\varepsilon_0 f} + \frac{\Delta\varepsilon \frac{f}{f_0}}{1 + \left(\frac{f}{f_0}\right)^2}.$$

The essential parameters in these two equations are the dipole density Δ and the mobility f_0 of the permanent electric dipole moments, because they are the main characteristics of the dispersion and the absorption curve of a tissue under inspection (see Figure 1).

The curve of $\varepsilon'(f)$ can be explained as follows: At low frequency, the dipoles can follow the alternating electromagnetic field; they can orientate themselves properly. This leads to a polarity of the tissue. With increasing frequency, due to the inertia of the dipole carrying

TABLE 1 Subject characteristics

	Number of included subjects	Histologically confirmed, absolute numbers (%)	Main areas	Mean age ± SD	Gender (female/male)
BCC	45	32 (61.5%)	head	75 ± 24	16 f/16 m
MM	14	9 (17.3%)	extremities and trunk	48 ± 37	3 f/6 m
SCC (Spinalioma)		5 (9.6%)	head	75 ± 18	2 f/3 m
Alternative findings		6 (11.5%)	head and extremities	62 ± 43	3 f/3 m
Excluded		7 (11.9%)	head	67 ± 18	2 f/5 m
Healthy volunteers	14	–	head, inner forearm	61 ± 22	11 f/3 m
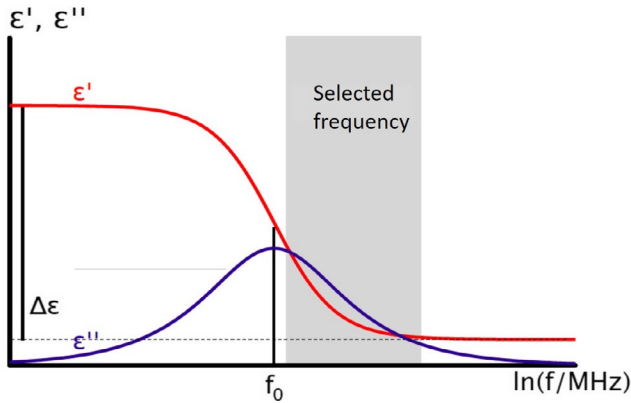
FIGURE 1 Graph of Debye's relations with dispersion ε' and absorption ε'', f_0 is the dipole mobility and $\Delta\varepsilon$ the dipole density. Gray shadowed is the selected frequency for the measurements [Colour figure can be viewed at wileyonlinelibrary.com]

tissue-cells, this is not possible anymore and the polarity decreases (see Figure 1).

To measure the complex dielectric constant, a transmitter feeds an electromagnetic wave into an open-ended coaxial probe, the cut inner and outer diameters forming a condenser in contact with the samples under test (Figure 2). The reflected wave is analyzed in comparison to the emitted wave, thus yielding the desired parameters Δ and f_0 depending on the investigated anatomical skin area.

The device used for the experiments was a ParaScan I (parelectrics). It is operated at a frequency range between 0.5 and 50 MHz . The measuring time is approx 20 seconds and the power are far below the high frequency permitted for application in humans. The legally permitted power limit is approximately 0.1 W, whereby ParaScan I is operated at approx 60 mW, which is by a factor of 2000 lower. The probe diameter is 2 cm, and the penetration depth of the wave is in the range of 0.5-1.0 mm.

Before this study started, the influences of pressure and water as a contact agent were investigated (data not shown). Preliminary investigations have shown that the dipole density and mobility
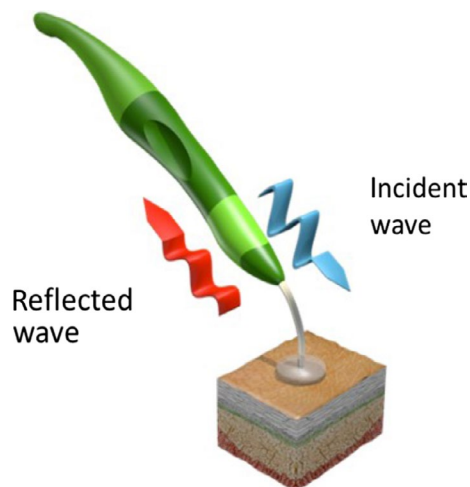
changes between anatomical regions of the body in healthy volunteers. Therefore, the difference between the lesion and an adjacent healthy area was calculated and used for the analysis.

2.3 | Measuring procedure

For documentation, at first a photo of the suspected lesion (BCC or MM) was taken.

Three independent and representative measurements of the lesion were performed using the parelectric device, followed by six measurements of unsuspicious skin in the vicinity (2 cm distance). The probe's diameter and geometry enables pressure control but limits the investigation to reachable areas.

If an adjacent skin area was not available, for example, in the face, a corresponding area of the other side on the face was taken as reference. For the measurements, a medium pressure was applied (the weight of probe exerting no additional pressure) to ensure good contact but avoiding blood vessel compression. The measurement is sensitive to the pressure exerted on the probe. Furthermore, a drop of water as an immersion liquid was applied.

The device was calibrated by means of an air measurement before each measurement to record possible temperature influences.

2.4 | Statistical analysis

Microsoft Excel 2010 and SPSS 22 (IBM® SPSS® Statistics) for Windows 2010 were used for statistical analyses. Data were analyzed by nonparametric, paired, and unpaired tests including, if appropriate, analysis of (co-)variance, Kruskal-Wallis test, Mann-Whitney, and Wilcoxon tests. The level of significance was assumed at $P \leq .05$.

3 | RESULTS

The results of the density and mobility data from unsuspicious skin at different body areas are shown in a cluster diagram in Figure 3. The data are mainly arranged in a hyperbolically shaped curve.
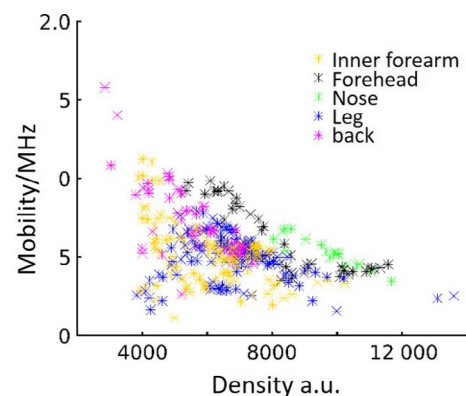

FIGURE 3 Cluster diagram of density and mobility of the dipoles in unsuspicious skin of different body areas [Colour figure can be viewed at wileyonlinelibrary.com]

FIGURE 2 Scheme of probe of the parelectric device [Colour figure can be viewed at wileyonlinelibrary.com]

The absolute values of both parameters differ strongly between the various skin areas and from subject to subject. To exclude such influences, the suspected lesions were normalized to the surrounding unsuspected skin.

The inclusion parameters were restricted to lesions suspected to be BCC and MM. In Figure 4, representative photographs taken with the integrated camera of confirmed BCC and MM are shown. The BCC clearly provides a non-homogenous structure. In addition, the MM is inhomogeneous but provides a clearer border to the surrounding normal skin.

In Figure 5, exemplary Debye curves of the selected frequency of unsuspected skin, BCC and MM are presented. The curves vary in shape and intensity. Nevertheless, also for the respective groups, the variations are high. Therefore, the mobility and density values were calculated relative to the surrounding healthy skin.

In Figure 6, the calculated relative mobility and relative density for the different tumor lesion and unsuspicious skin are presented. Beside BCC and MM, SCC has been included in the analysis because the histopathological findings resulted in five SCC instead of MM and BCC. Data from seven patients were excluded because the probe could not be perfectly attached or air was between probe and

skin, the lesion was sublime and encrusted, or the anamnesis was conspicuous, and the measured data were not valid.

The data from the unsuspicious skin (control) show a low variance around the value 1 for relative mobility. For relative density, the median of normal skin is below 1 and the variance is higher compared to the data of mobility. The data of all tumor groups show a high variance independent of the tumor entity. All relative mobility medians are higher than 1 and all relative density medians lower than 1. The relative mobility for normal skin is significantly lower than for BCC, MM, and SCC. The significance between the tumor values and normal skin differs, which could be related to the number of measurements. Nevertheless, the difference between normal skin and the five data points for SCC was significant ($P = .05$).

The relative densities of BCC, MM, and SCC are not significantly higher compared to normal skin, but for BCC and SCC the differences showed a trend, $P \leq .1$. No differences between tumor groups could be found for both parelectric parameters.

Comparing pooled data of all tumor entities with normal skin both parameters, relative density and relative mobility, are significantly different (Figure 7). For relative mobility, the differences to normal skin are even highly significant ($P \leq .01$). These data also illustrate

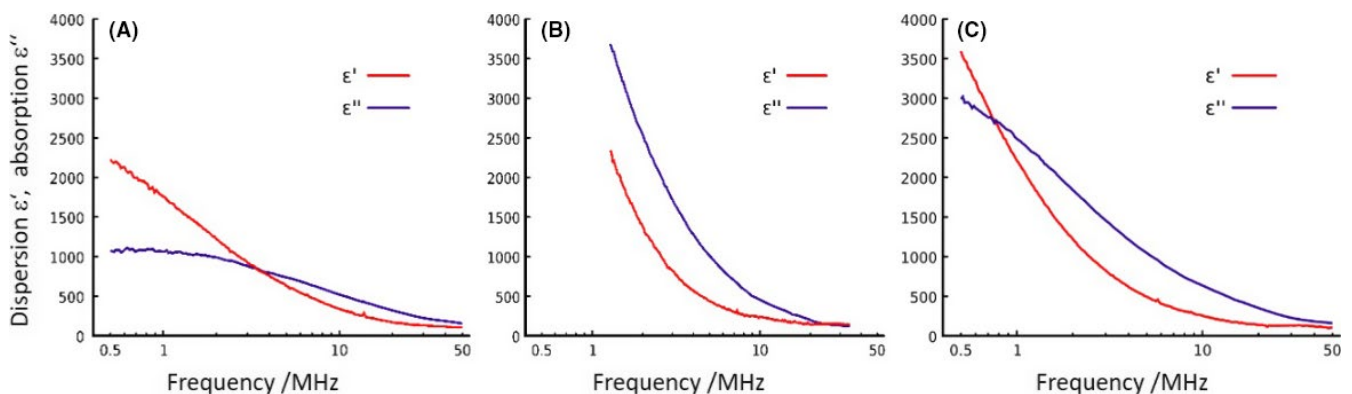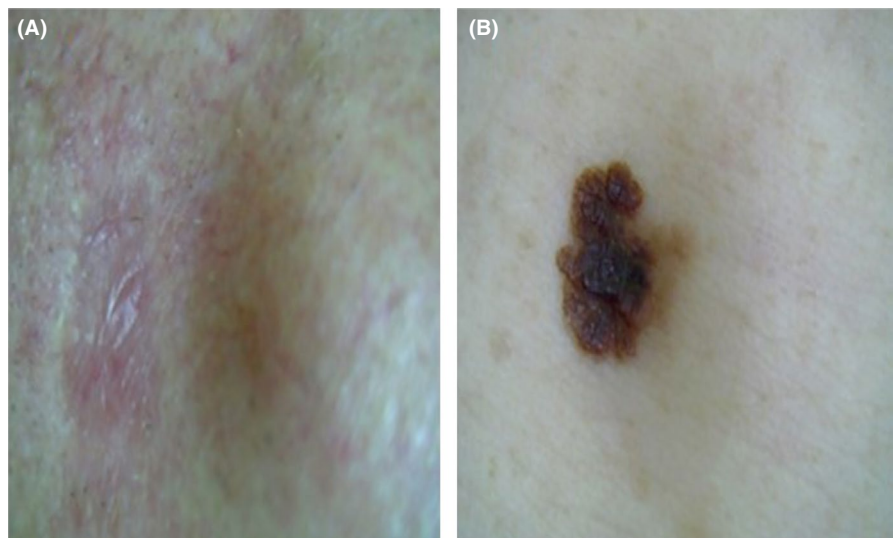**FIGURE 4** Selected photographs of (A) BCC and (B) MM from two different patients

FIGURE 5 Debye curves with dispersion ′ and absorption ″ for A) unsuspicious skin at the inner forearm of a patient, B) BCC at the cheek and C) MM at the lower abdomen
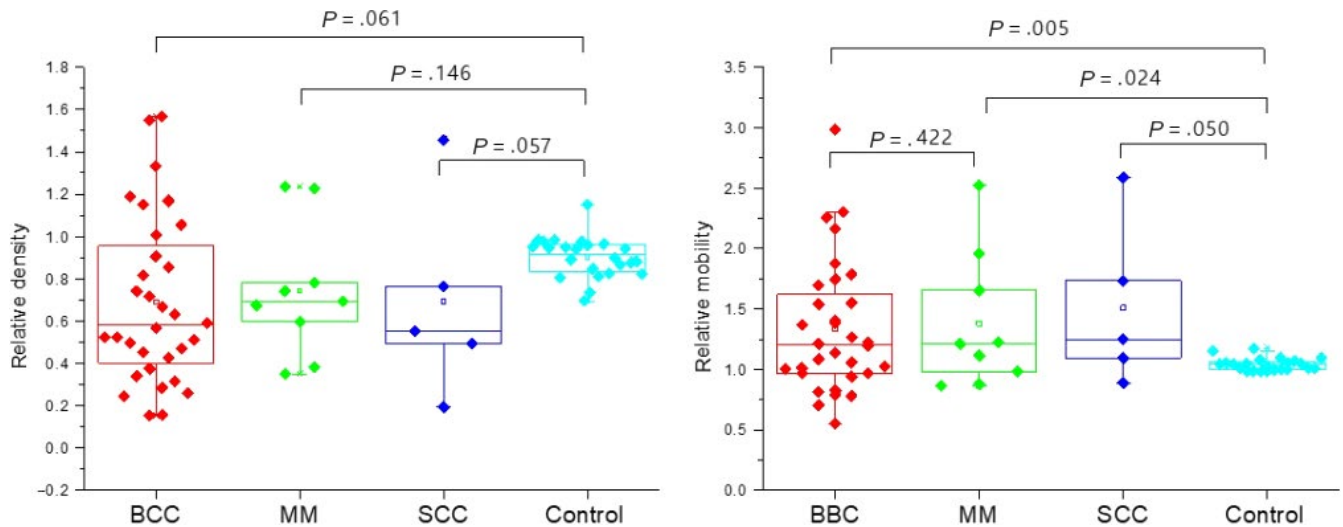
FIGURE 6 Boxplot of relative density (left) and mobility (right) for the different tumor groups and control skin [Colour figure can be viewed at wileyonlinelibrary.com]
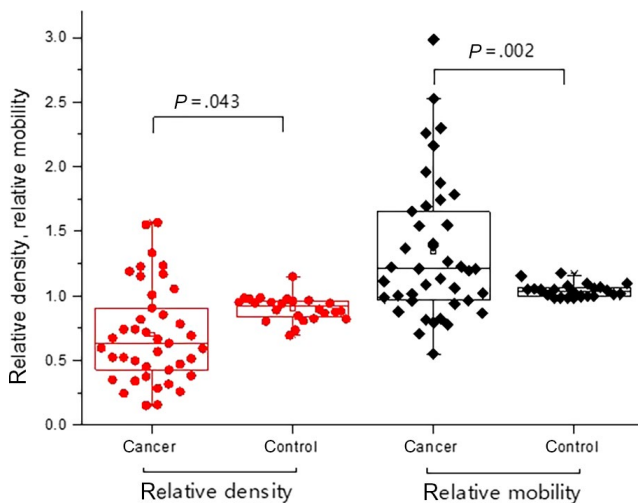

FIGURE 7 Boxplot for relative mobility and relative density using all tumor data and the corresponding normal skin data [Colour figure can be viewed at wileyonlinelibrary.com]

the higher variation for mobility compared to the density values in tumors.

Another way of analyzing the data is using a cluster diagram as shown in Figure 3 for different normal skin areas. Figure 8 A shows the cluster diagram of all relative tumor data and the corresponding relative normal data. The variance of normal data in this diagram is low and they cluster around 1:1. Figure 8 B provides an enlarged detail of graph A, and the circle illustrates a possible cluster of mainly normal skin data. It includes three BCC and one SCC as false-negative data.

4 | DISCUSSION

This first pilot study using non-invasive parelectric spectroscopy for skin tumor discrimination has shown high variations for dipole

mobility and density for normal unsuspicious skin at different skin areas.

Non-invasive parelectric spectroscopy determines specific electrical properties and structural changes of the tissue. Permanent electrical dipoles align themselves, for example, on cell membranes under the influence of an external alternating field and form a polarization in response, which is measured with a coaxial probe. The parelectric parameters calculated from the polarization, such as dipole density and dipole motion, as well as the polarization, are influenced by the tissue structure and the factors acting on it.

The measured dipoles could be associated with water molecules, which are ubiquitous in the skin and phospholipids, which are components in most of the cell membranes but also located in the stratum corneum.[17] The human skin can be divided microscopically into epidermis (stratum corneum, stratum lucidum, stratum granulosum, stratum spinosum, and stratum basale), dermis (stratum papillare and stratum reticulare), and subcutis. Depending on the location, the thickness of the skin varies from 1.5 to 4 mm.[18] Epithelial cells densely pack the epidermis to a depth of between 75 and 150 μm (up to 600 μm thick on palms/soles). The dermis is usually <2 mm thick, but maybe up to 4 mm thick (eg, adult back) and provides most of the mechanical strength to the skin. Variation in the parelectic parameters might be related to different thickness of skin layers at different areas and individual skin tissue components. This is in agreement with other non-invasive investigations using optical coherence tomography (OCT), multiphoton tomography (MPT), and Raman spectroscopy which have shown differences for the thickness of epidermis and the stratum corneum, the size and number of hair follicles, sweat gland density and the skin tissue components.[19-22]

In order to exclude skin area variations, the measured absolute values of skin tumor lesions were normalized to the unsuspicious nearby skin or exactly corresponding skin of the other side of the
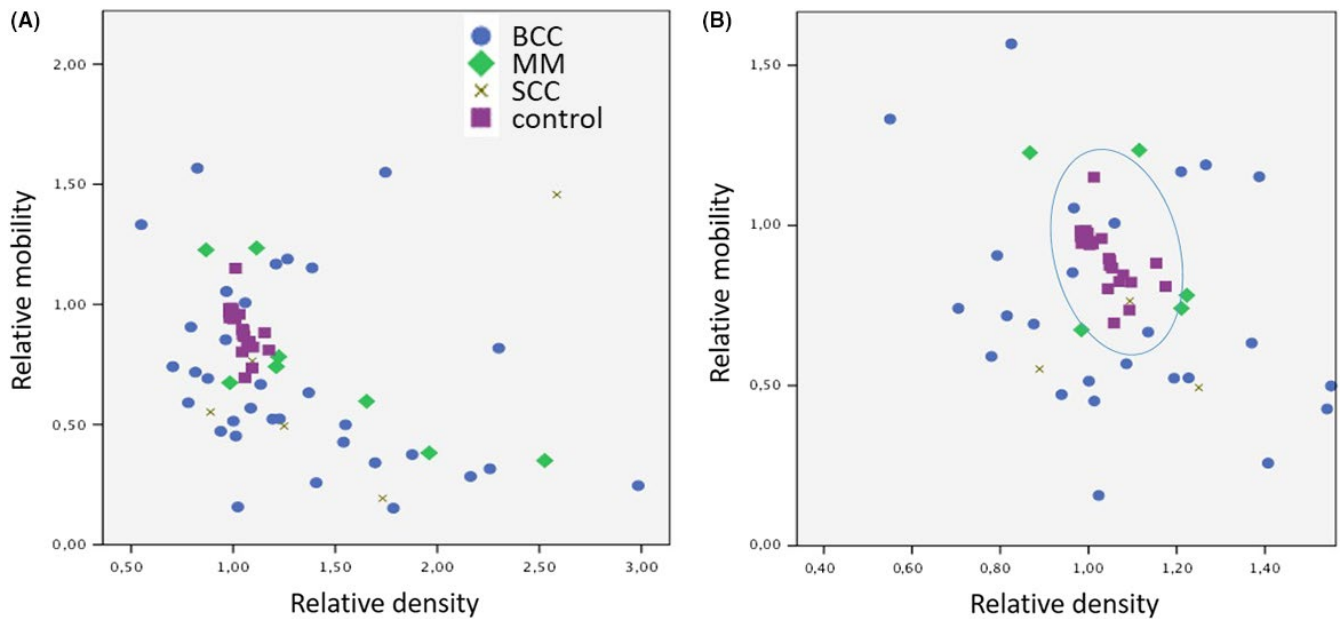
FIGURE 8 Cluster diagram of relative density and mobility for BCC, MM, SCC, and unsuspicious skin A) all data, B) selected data at the border to unsuspicious control skin [Colour figure can be viewed at wileyonlinelibrary.com]

body. Such procedure has been applied also for other spectroscopic methods such as Raman spectroscopy to detect skin cancer.[7]

The results of relative mobility and density of the tumor lesions compared to normal skin indicate different skin structures or compositions in skin tumors. The relative mobility showed higher values and significantly higher differences to normal skin compared to the other parameter relative density. The density of the tumor lesion decreases and the mobility increases. This could be associated with more free mobile water molecules in the skin as shown by Raman spectroscopic investigations, attributing different mobilities of water molecules to the different strengths of hydrogen bonds.[23]

Our results are in agreement with optical measurements such as OCT which is based on refractive index differences of the different skin layers and structures. Skin tumors are associated with other refractive indices and provide different gray values. The refractive index can be related to different densities of tissue. Also with OCT tumor types are difficult to distinguish.[24]

Parelectric spectroscopy has shown to be able to differentiate between normal and cancerous tissue and organs in mice and human laryngeal tissue.[14,15] Nevertheless, a sensitivity to detect differences between skin tumor types was not achieved.

5 | CONCLUSION

The investigation has shown that the values for mobility and density of dipoles provide a high variance depending on the body area. Furthermore, mobility of the dipoles in skin cancer is stronger altered than the density. The results of the pilot study indicate that the parelectric spectroscopy might be an additional, useful non-invasive diagnostic procedure to distinguish between normal skin and skin cancer, but is not capable of distinguishing between different

types of skin cancer. Therefore, the type of skin cancer should still be differentiated by biopsies, which are also necessary for skin cancer deeper than 1mm because spectroscopic measurements cannot penetrate into deeper parts of the skin.

CONFLICT OF INTEREST

The authors have no conflict of interest to declare.

ORCID

Martina C. Meinke https://orcid.org/0000-0002-3937-9906

REFERENCES

1. Mebed AH, Soliman HO, Gad ZS, Abdel Hay RM. Multimodality treatment for non melanoma skin cancer: a prospective study done on 120 Egyptian patients. *J Egypt Natl Canc Inst*. 2010;22:49-55.
2. Walls B, Jordan L, Diaz L, Miller R. Targeted therapy for cutaneous oncology: a review of novel treatment options for non-melanoma skin cancer: part II. *J Drugs Dermatol*. 2014;13:955-958.
3. Walls B, Jordan L, Diaz L, Miller R. Targeted therapy for cutaneous oncology: a review of novel treatment options for non-melanoma skin cancer: part I. *J Drugs Dermatol*. 2014;13:947-952.
4. Holmes J, von Braunmuhl T, Berking C, et al. Optical coherence tomography of basal cell carcinoma: influence of location, subtype, observer variability and image quality on diagnostic performance. *Br J Dermatol*. 2018;178:1102–1110.
5. Ulrich M, Klemp M, Darvin ME, Konig K, Lademann J, Meinke MC. In vivo detection of basal cell carcinoma: comparison of a reflectance confocal microscope and a multiphoton tomograph. *J Biomed Opt*. 2013;18:61229.
6. de Leeuw J, van der Beek N, Neugebauer WD, Bjerring P, Neumann HA. Fluorescence detection and diagnosis of non-melanoma skin cancer at an early stage. *Lasers Surg Med*. 2009;41:96-103.

7. Schleusener J, Gluszczynska P, Reble C, et al. In vivo study for the discrimination of cancerous and normal skin using fibre probe-based Raman spectroscopy. *Exp Dermatol*. 2015;24:767-772.

8. Heuke S, Vogler N, Meyer T, et al. Detection and discrimination of non-melanoma skin cancer by multimodal imaging. *Healthcare (Basel)*. 2013;1:64-83.

9. Ra H, Gonzalez-Gonzalez E, Uddin MJ, et al. Detection of non-melanoma skin cancer by in vivo fluorescence imaging with fluorocoxib A. *Neoplasia*. 2015;17:201-207.

10. Blaschke T, Kankate L, Kramer KD. Structure and dynamics of drug-carrier systems as studied by parelectric spectroscopy. *Adv Drug Deliv Rev*. 2007;59:403-410.

11. Sivaramakrishnan R, Kankate L, Niehus H, Kramer KD. Parelectric spectroscopy of drug-carrier-systems–distribution of carrier masses or activation energies. *Biophys Chem*. 2005;114:221-228.

12. Sivaramakrishnan R, Nakamura C, Mehnert W, Korting HC, Kramer KD, Schafer-Korting M. Glucocorticoid entrapment into lipid carriers–characterisation by parelectric spectroscopy and influence on dermal uptake. *J Control Release*. 2004;97:493-502.

13. Braem C, Blaschke T, Panek-Minkin G, et al. Interaction of drug molecules with carrier systems as studied by parelectric spectroscopy and electron spin resonance. *J Control Release*. 2007;119:128-135.

14. Blaschke T, Sivaramakrishnan R, Gross M, Kramer KD. Organ mapping using parelectric spectroscopy. *Phys Med Biol*. 2006;51:1623–1631.

15. Mahlstedt K, Blaschke T, Kramer KD, Gross M. Parelectric spectroscopy for noninvasive diagnosis of laryngeal tissue. *Biomed Tech (Berl)*. 2002;47:70-75.

16. Debye P. Interferrometric determination of structure of single molecules. *Z Elktrochem Angew P*. 1930;36:612-615.

17. Paul T, Saha J. Effect of head group orientation on phospholipid assembly. *Phys Rev E*. 2017;95:062703.

18. Terhorst D. *Basics Dermatologie*. München: Elsevier, Urban & FischerVerlag; 2009.

19. Czekalla C, Schonborn KH, Lademann J, Meinke MC. Noninvasive determination of epidermal and stratum corneum thickness in vivo using two-photon microscopy and optical coherence tomography: impact of body area, age, and gender. *Skin Pharmacol Phys*. 2019;32:142-150.

20. Otberg N, Richter H, Schaefer H, Blume-Peytavi U, Sterry W, Lademann J. Variations of hair follicle size and distribution in different body sites. *J Invest Dermatol*. 2004;122:14-19.

21. Czekalla C, Schonborn KH, Doge N, et al. Impact of body site, age, and gender on the collagen/elastin index by noninvasive in vivo vertical two-photon microscopy. *Skin Pharmacol Physiol*. 2017;30:260-267.

22. Lee M, Won K, Kim EJ, Hwang JS, Lee HK. Comparison of stratum corneum thickness between two proposed methods of calculation using Raman spectroscopic depth profiling of skin water content. *Skin Res Technol*. 2018;24:504-508.

23. Sdobnov AY, Darvin ME, Schleusener J, Lademann J, Tuchin VV. Hydrogen bound water profiles in the skin influenced by optical clearing molecular agents-Quantitative analysis using confocal Raman microscopy. *J Biophotonics*. 2018;12:e201800283.

24. Batz S, Wahrlich C, Alawi A, Ulrich M, Lademann J. Differentiation of different nonmelanoma skin cancer types using OCT. *Skin Pharmacol Physiol*. 2018;31:238-245.